PROCEEDINGS OF SCIENCE

ONLINE ICRC 2021
THE ASTROPARTICLE PHYSICS CONFERENCE
Berlin | Germany
37th International Cosmic Ray Conference
12–23 July 2021

Precise Measurement of the Cosmic-Ray Electron and Positron Spectrum with CALET on the International Space Station

Shoji Torii[a,*] **and Yosui Akaike**[a] **on behalf of the CALET Collaboration**
(a complete list of authors can be found at the end of the proceedings)

[a] *Waseda Research Institute for Science and Engineering, Waseda University,*
17 Kikuicho, Shinjuku, Tokyo, Japan
E-mail: torii.shoji@waseda.jp, yakaike@aoni.waseda.jp

Primary objectives of the CALET (CALorimetric Electron Telescope) mission are to search for possible nearby cosmic-ray sources and dark matter signatures with the precise measurement of the electron and positron (all-electron) spectrum. The instrument, consisting of a charge detector, an imaging calorimeter and a total absorption calorimeter, is optimized to measure the all-electron spectrum well into the TeV region with a thick calorimeter of 30 radiation length with fine shower-imaging capability. Due to the excellent energy resolution (a few % above 10 GeV) and the outstanding e/p separation ($\sim 10^5$), CALET achieves optimal performance for a detailed search for structures in the energy spectrum. CALET has been accumulating scientific data for more than five years without any major interruption, and the statistics of observed electron events has increased more than double since the latest publication in 2018. In this paper we will present precise measurements of the all-electron spectrum up to several TeV, as obtained with the high statistics data, and we will briefly discuss about its interpretation.

37th International Cosmic Ray Conference (ICRC 2021)
July 12th – 23rd, 2021
Online – Berlin, Germany

*Presenter

1. Introduction

High-energy cosmic-ray electrons provide a unique probe of nearby cosmic accelerators. Electrons rapidly lose energy via inverse Compton scattering and synchrotron emission during propagation in the Galaxy. Since their diffusion distance above 1 TeV is limited to less than 1 kpc, only a few super nova remnants as potential TeV sources are located in the vicinity of the Solar System. A precise measurement of the electron spectrum in the TeV region might reveal interesting spectral features to provide the first experimental evidence of the possible presence of a nearby cosmic-ray source [1, 2].

In addition, the apparent increase of the positron fraction over 10 GeV established by Payload for Antimatter Matter Exploration and Light nuclei Astrophysics (PAMELA) [3] and the Alpha Magnetic Spectrometer (AMS-02) [4] may require a primary source component of the positrons in addition to the generally accepted secondary origin. Candidates for such primary sources range from astrophysical (pulsar) to exotic (dark matter). Since these primary sources emit electron-positron pairs, it is expected that the all-electron (electrons and positrons) spectrum would exhibit a spectral feature due to the primary source component of electrons and positrons, in the corresponding energy range above 10 GeV.

The Calorimetric Electron Telescope (CALET) is a space experiment on the International Space Station (ISS) for long term observations of cosmic-rays, which is optimized for the measurement of the all-electron spectrum [5]. It was launched on August 19, 2015 with the Japanese carrier H-IIB, delivered to the ISS by the HTV-5 Transfer Vehicle, and installed on the Japanese Experiment Module - Exposed Facility (JEM-EF). The first result of the all-electron spectrum was published in the energy range from 10 GeV to 3 TeV as the world's first space observation up to the TeV region [6]. Subsequently, the updated spectrum was published with statistics larger by a factor of $\sim$2 compared to the first by using more than 2 years of flight data and the full geometrical acceptance in the high-energy region [7]. The energy range is extended to 4.8 TeV, and the observed spectrum shows a suppression of the flux above 1 TeV, compatible with the DAMPE result [8]. In this paper, we present a preliminary CALET all-electron spectrum obtained from observations over $\sim$5 years with statistics increased furthermore by a factor of $\sim$2.3 since the last publication [7]. The result is compared with other observations, and a plausible interpretation is briefly discussed with its tentative spectral fitting in the 10 GeV-4.8 TeV range including a possible contribution from pulsars and the Vela SNR.

2. Instrument

CALET employs a fully active calorimeter with thirty radiation-length thickness for particles at normal incidence. It consists of a charge detector (CHD), a three radiation-length thick imaging calorimeter (IMC), and a twenty-seven radiation-length thick total absorption calorimeter (TASC). It has a field of view of $\sim$45° from zenith and a geometrical factor of $\sim$ 1,040 cm^2 sr for high-energy electrons. CHD, which identifies the charge of the incident particle, is comprised of a pair of plastic scintillator hodoscopes arranged in two orthogonal layers. IMC is a sampling calorimeter alternating thin layers of Tungsten absorber, optimized in thickness and position, with layers of

scintillating fibers read-out individually. TASC is a tightly packed lead-tungstate (PbWO4; PWO) hodoscope, capable of almost complete absorption of the TeV-electron showers.

Figure 1 shows a 3.05 TeV-electron candidate and a proton candidate with comparable energy deposit (2.89 TeV) in the detector. Compared to hadron showers, which have significant leakage, the containment of the electromagnetic shower creates a difference in shower shape, especially in the bottom part of TASC, allowing for an accurate electron identification in the presence of a large hadron background. Together with the precision energy measurements from total absorption of electromagnetic showers, it is possible to derive the electron spectrum well into the TeV region with a straightforward and reliable analysis.

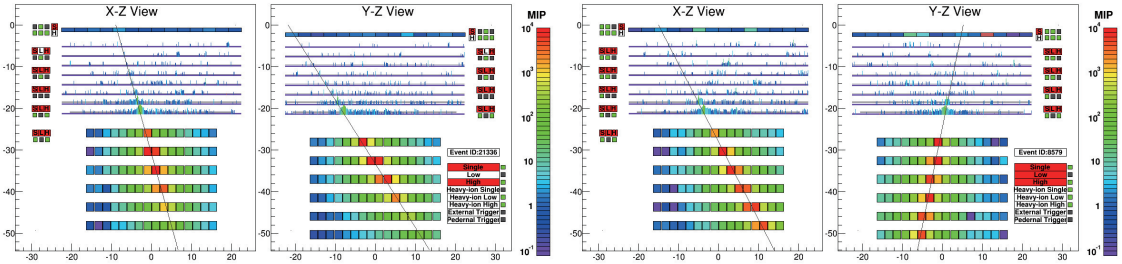

Figure 1: Examples of TeV event candidates showing energy deposit in each detector channel in the X Z and Y Z views. Left: An electron (or positron) candidate (reconstructed energy of 3.05 TeV and energy deposit sum of 2.89 TeV). Right: A proton candidate (energy deposit sum of 2.89 TeV).

3. Observation and Detector Performance

Since the start of scientific observations on October 13, 2015, smooth and continuous operations have being taken place. The live time fraction is considerably high being 86 % without any interruption of observation by unexpected accidents. Fig. 2 shows the time profile of the real time and the live time of the observations [9].

While excellent energy resolution inside the TeV region is one of the most important features of a thick calorimeter instrument like CALET, calibration errors must be carefully assessed and taken into account in the estimation of the actual energy resolution. Our energy calibration includes the evaluation of the conversion factors between analog-to-digital converter units and energy deposits, ensuring linearity over each gain range (TASC has four gain ranges for each channel), and provides a seamless transition between neighboring gain ranges [10]. Temporal gain variations occurring during long time observations are also corrected in the calibration procedure. The errors at each calibration step, such as the correction of position and temperature dependence, consistency between energy deposit peaks of non-interacting protons and helium, linear fit error of each gain range, and gain ratio measurements, as well as slope extrapolation, are included in the estimation of the energy resolution. As a result, a very high resolution of 2% or better is achieved above 20 GeV [10]. Moreover, the very large dynamic range of the energy measurement as presented in Fig. 3 is confirmed without saturation of measured energy up to 1 PeV for deposit energy in TASC. These spectra are checked monthly to confirm the stability of the extrapolation using four gain ranges.

It should be noted that, even with such a detailed calibration, the determining factor for the energy resolution is the calibration uncertainty, as the intrinsic resolution of CALET is $\sim$1% . Intrinsic resolution refers to the detector's capability by design, taking advantage of the thick, fully

active total absorption calorimeter. Also important is the fact that the calibration error in the lower gain ranges is crucial for the spectrum measurements in the TeV range.

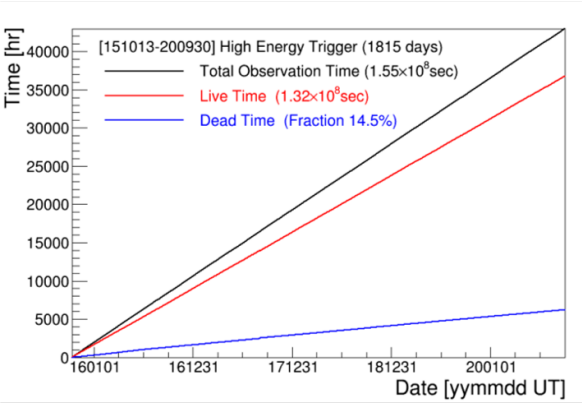

Figure 2: Time dependences of the accumulated real time and live time of the observations since Dec. 2015

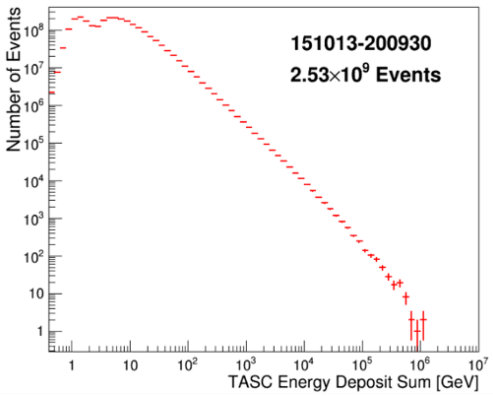

Figure 3: Observed spectrum of the energies deposited in TASC after calibrations.

4. Data Analysis

In this paper, we report the results obtained by analysis of 1815 days of flight data collected with a high-energy shower trigger [9]. The analysis has been carried out for the observed events in the full detector acceptance, by a similar procedure as described in Ref. [7]. A Monte Carlo (MC) program was used to simulate physics processes and detector response based on the simulation package EPICS [11] (EPICS9.20/COSMOS8.00). Using MC event samples of electrons and protons, event selection and event reconstruction efficiencies, energy correction factor, and background contamination were derived. An independent analysis based on GEANT4 [12] was performed, and small differences between the MC models are included in the systematic uncertainties. The GEANT4 simulation employs the hadronic interaction models FTFP_BERT as the physics list, while DPMJET3 [13] is chosen as the hadronic interaction model in the EPICS simulation.

We use the "electromagnetic shower tracking" algorithm [14] to reconstruct the shower axis of each event, taking advantage of the electromagnetic shower shape and IMC design concept. As input for the electron identification, well-reconstructed and well-contained single-charged events are preselected by (1) an off-line trigger confirmation, (2) a geometrical condition, (3) a track quality cut to ensure reconstruction accuracy, (4) a charge selection using CHD, (5) having a longitudinal shower development, and (6) a lateral shower containment consistent with those expected for electromagnetic cascades.

In addition to fully contained events, the events incident from the IMC sides and exiting through the sides of TASC are used for analysis. For events not crossing the CHD, we use the energy deposit of the first hit IMC layer to determine their charge. The path length inside TASC is required to be longer than that of vertical depth of TASC, i.e. twenty-seven radiation lengths.

The energy of incident electrons is reconstructed using the energy correction function, which converts the energy deposit information of TASC and IMC into primary energy for each geometrical condition. In order to identify electrons and to study systematic uncertainties in the electron

identification, we applied two methods: a simple two-parameter cut and a multivariate analysis based on boosted decision trees (BDTs).

Calculation of event selection efficiencies, BDT training, and estimation of proton background contamination are carried out separately for each geometrical condition and combined in the end to obtain the final spectrum. Considering the fact that the lower energy region is dominated by systematics in our analysis, and therefore more statistics would not significantly improve the precision of our data, only the fully-contained events are included in the lower energy region below 475 GeV. Examples of a BDT response distribution including all acceptance conditions are shown in Fig. 4. In the final electron sample, the resultant contamination ratios of protons are ~5 % up to 1 TeV, and 10% - 20% in the 1 - 4.8 TeV region, while keeping a constant high efficiency of 80 % for electrons.

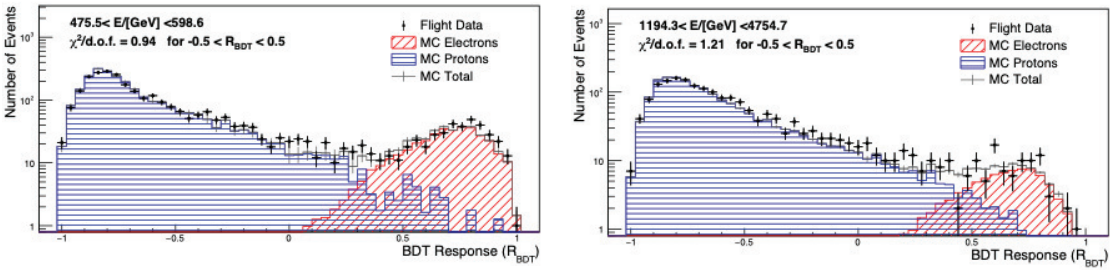

Figure 4: Examples of BDT response distributions in the 476 < E < 599 GeV bin (left) and in the highest region energy , 1196 < E < 4755 GeV bin. (left), including all acceptance conditions .

The absolute energy scale was calibrated and shifted by + 3.5% [6] as a result of a study of the geomagnetic cutoff energy. Since the full dynamic range calibration [10] was carried out with a scale-free method, its validity holds regardless of the absolute scale uncertainty.

The systematic uncertainties are described in details at Ref. [15] and an accompanied paper in this conference [16]

5. Electron + Positron Spectrum

Figure 5 shows the extended electron and positron spectrum in this analysis using the observed events with statistics increased by a factor of 2.3 since the last publication [7]. The error bars along horizontal and vertical axes indicate bin width and statistical errors, respectively. The gray band is representative of the quadratic sum of statistical and systematic errors, using the same definition as the one given in Ref. [6]. Systematic errors include errors in the absolute normalization and energy dependent ones, except for the energy scale uncertainty. The energy dependent errors include those obtained from BDT stability, trigger efficiency in the low-energy region, tracking dependence, dependence on methods of charge identification, and of electron identification, as well as MC model dependence. In more refined interpretation studies, the latter four contributions and normalization could be treated by including their weights as nuisance parameters, while the first two components must be added in quadrature to the statistical errors. Conservatively, all of them are included in the total error estimate in Fig. 5.

Comparing with other recent experiments in space (AMS-02, Fermi Large Area Telescope (Fermi-LAT), and DAMPE), our spectrum shows good agreement with AMS-02 data below 1 TeV.

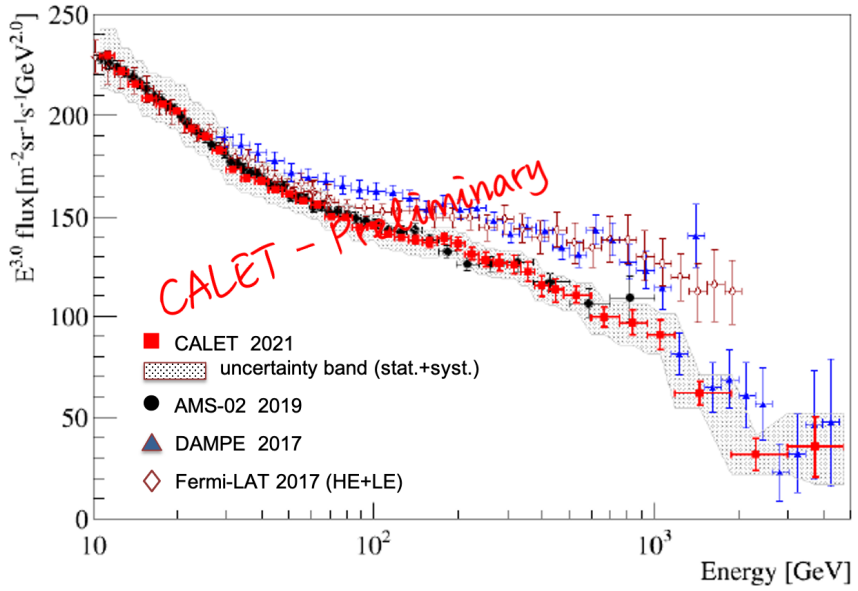

Figure 5: Cosmic-ray all-electron spectrum measured by CALET from 11 GeV to 4.8 TeV using the same energy binning as in our previous publication [7], where the gray band indicates the quadratic sum of statistical and systematic errors (not including the uncertainty on the energy scale). Also plotted are direct measurements in space [8, 17–19] for comparison.

In the energy region from 40 to 300 GeV, the power-law index of CALET's spectrum is found to be -3.128±0.019, which is consistent with other experiments within errors. However, the spectrum is considerably softer from 300 to 600 GeV than the spectra measured by DAMPE and Fermi-LAT. The CALET results exhibit a lower flux than those of DAMPE and Fermi-LAT from 300 GeV up to near 1 TeV, indicating the presence of unknown systematic effects.

To check if the CALET spectrum is consistent with a possible break at 0.9 TeV, as suggested by DAMPE's observations, we have adopted exactly the same energy binning as DAMPE to show our spectrum. In Fig. 6, we fit our spectrum with a smoothly broken power-law model [8] in the energy range from 55 GeV to 4.8 TeV, while fixing the break energy at 914 GeV(blue line). A broken power law steepening from -3.151 ±0.012 by -0.873±0.178 fits our data well, with χ^2 = 11.64 and number of degrees of freedom (NDF) equal to 29. This result is consistent with DAMPE regarding the spectral index change of 0.7±0.3. A single power-law fit over the same energy range (black line) gives an index -3.197±0.011 with χ^2 /NDF=54.50/30, which means that the broken power law is favored with 6.55 sigma significance over the single power law. An exponentially cut-off power law [20] (green line) is also presented for comparison, which has the power index of -3.054±0.026 below a cutoff energy of 2170 GeV± 340 GeV with χ^2 /NDF =11.25/29 which gives a significance of σ=6.58 over the single power law.

On the other hand, as presented in Fig. 6, the flux in the 1.4 TeV bin of DAMPE's spectrum, which might imply a peak structure, is not compatible with CALET results at a level of > 4 sigma significance, including the systematic errors from both experiments.

Here, we try to explain the CALET energy spectrum observed in a whole energy region. Figure 7 presents one example of fitting a model for the electron and positron origins described in

§1. The positron flux of AMS-02 is fitted by contribution from secondaries (red dashed line) + several pulsars (dashed-dotted line), and the electron flux is fitted by secondaries + distant SNRs (black dashed line) with cut-off at 1 TeV. As the dominating source above 1 TeV, we assume a possible contribution from the Vela SNR (green line), which is explained by energy output of 2.08 x 10^{48} erg in electron CR above 1 GeV. The spectra by Vela and secondaries (e^-,e^+) are calculated with the numerical propagation code DRAGON [21], which is also used to define the propagation parameters via calculation of the nuclei spectra, concurrently providing spectra of the secondary electrons and positrons forming part of the background [22]. The details of this whole-region interpretation of the all-electron spectrum and its implications of the nearby source contribution are explained in Ref. [22]. However, for the highly desired goal of getting conclusive information of the nearby source contribution in the TeV region, we need still to extend the energy spectrum up to 20 TeV with much more statistics.

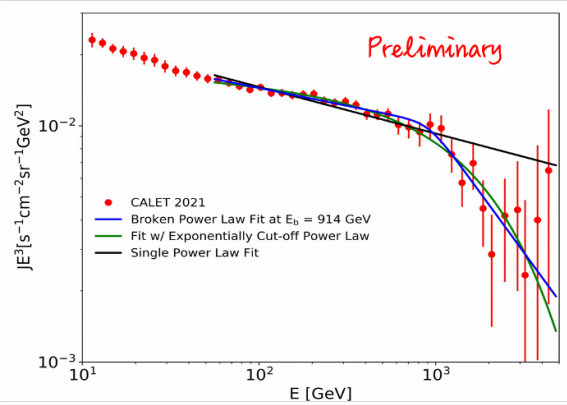

Figure 6: All-electron spectrum measured by CALET from 11 GeV to 4.8 TeV using the same energy binning as DAMPE's result [8]. See text for details of fittings.

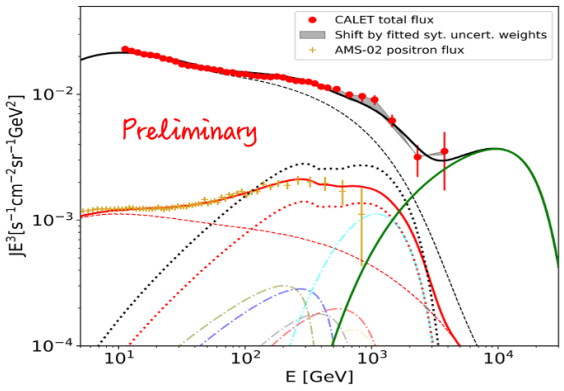

Figure 7: Tentative spectral fit over a whole region of the CALET observations including the pulsars and the Vela SNR above 1 TeV. See details in text.

6. Summary and Future Prospects

We have extended our previous result [7] of the CALET all-electron spectrum with an approximate increase by a factor of 2.3 of the statistics. The data in the TeV region show a suppression of the flux compatible with the DAMPE results, and the accuracy of the break's sharpness and position, and of the spectral shape above 1 TeV, are improved by the better statistics. The CALET observations on the ISS approved to continue up to 2024 (at least) will bring further increase of the statistics and reduction of the systematic errors based on the analysis. By specifying the breakdown of systematic uncertainties, our extended all-electron spectrum together with the AMS-02 positron flux measurement provides essential information to investigate spectral features in the framework of nearby SNRs and pulsars and/or dark matter inspired models.

7. Acknowledgements

We gratefully acknowledge JAXA's contributions to the development of CALET and to the operations onboard the International Space Station. We also wish to express our sincere gratitude

to ASI and NASA for their support of the CALET project. This work was supported in part by a JSPS Grant-in-Aid for Scientific Research (S)(No. 19H05608) and (C) 21K03592.

References

[1] J. Nishimura, *et al*., Astrophys. J. 238, 394 (1980).

[2] T. Kobayashi, Y.Komori, K.Yoshida, and J.Nishimura, Astrophys. J. 601, 340 (2004).

[3] O. Adriani, *et al*. (PAMELA Collaboration) , Nature (London) 458, 607 (2009).

[4] L. Accardo, *et al*. (AMS-02 Collaboration), Phys. Rev. Lett. 113, 121101 (2014).

[5] S. Torii and P.S.Marrocchesi, *et al*. (CALET Collaboration), Advances in Space Research 64 (2019) 2531-2537.

[6] O. Adriani, *et al*. (CALET Collaboration), Phys. Rev. Lett. 119, 181101 (2017).

[7] O. Adriani, *et al*. (CALET Collaboration), Phys. Rev. Lett. 120, 261102 (2018).

[8] G. Ambrosi, *et al*. (DAMPE Collaboration) , Nature (London) 552, 63 (2017).

[9] Y.Asaoka, Y.Ozawa, S.Torii *et al*. (CALET Collaboration), Atroparticle Physics 100, 29 (2018).

[10] Y. Asaoka, Y. Akaike, Y. Komiya, R. Miyata, S. Torii, *et al*. (CALET Collaboration), Astropart. Phys. 91, 1 (2017).

[11] K.Kasahara, EPICS, http://cosmos.n.kanagawa-u.ac.jp/EPICSHome/.

[12] S. Agostinelli, *et al*., Nucl. Instrum. Methods Phys. Res., Sect. A 506, 250 (2003).

[13] S. Roesler, R. Engel, and J. Ranft, DPMJET3, http://sroesler.web.cern.ch/sroesler/dpmjet3.html.

[14] Y. Akaike, *etal*. (CALET Collaboration), in Proceedings of 33rd International Cosmic Ray Conference (ICRC2013) 726 (2013).

[15] O. Adriani, *et al*. (CALET Collaboration), Phys. Rev. Lett. 120, 261102 (2018) Supplement Material.

[16] E. Berti, L. Patini, Y. Akaike *et al*. (CALET Collaboration), Poster ♯ 628 in this conference.

[17] O. Adriani, *et al*. (PAMELA Collaboration), Riv. Nuovo Cimento 40, 473 (2017).

[18] M. Aguilar, *et al*. (AMS-02 Collaboration), Phys. Rev. Lett. 122, 101101 (2019).

[19] M. Aguilar, *et al*. (Fermi Collaboration), Phys. Rev. Lett. 113, 221102 (2014).

[20] S. Abdollahi, *et al*., Phys. Rev. D 95, 082007 (2017).

[21] D. Gaggero, et al., Phys. Rev. Lett. 111, 021102 (2013).

[22] H. Motz *et al*. (CALET Collaboration), Poster ♯ 492 in this conference.

Full Authors List: CALET Collaboration

O. Adriani[1,2], Y. Akaike[3,4], K. Asano[5], Y. Asaoka[5], E. Berti[1,2], G. Bigongiari[6,7], W. R. Binns[8], M. Bongi[1,2], P. Brogi[6,7], A. Bruno[9,10], J. H. Buckley[8], N. Cannady[11,12,13], G. Castellini[14], C. Checchia[6], M. L. Cherry[15], G. Collazuol[16,17], K. Ebisawa[18], A. W. Ficklin[15], H. Fuke[18], S. Gonzi[1,2], T. G. Guzik[15], T. Hams[11], K. Hibino[19], M. Ichimura[20], K. Ioka[21], W. Ishizaki[5], M. H. Israel[8], K. Kasahara[22], J. Kataoka[23], R. Kataoka[24], Y. Katayose[25], C. Kato[26], N. Kawanaka[27,28], Y. Kawakubo[15], K. Kobayashi[3,4], K. Kohri[29], H. S. Krawczynski[8], J. F. Krizmanic[11,12,13], P. Maestro[6,7], P. S. Marrocchesi[6,7], A. M. Messineo[30,7], J.W. Mitchell[12], S. Miyake[32], A. A. Moiseev[33,12,13], M. Mori[34], N. Mori[2], H. M. Motz[35], K. Munakata[26], S. Nakahira[18], J. Nishimura[18], G. A. de Nolfo[9], S. Okuno[19], J. F. Ormes[36], N. Ospina[16,17], S. Ozawa[37], L. Pacini[1,14,2], P. Papini[2], B. F. Rauch[8], S. B. Ricciarini[14,2], K. Sakai[11,12,13], T. Sakamoto[38], M. Sasaki[33,12,13], Y. Shimizu[19], A. Shiomi[39], P. Spillantini[1], F. Stolzi[6,7], S. Sugita[38], A. Sulaj[6,7], M. Takita[5], T. Tamura[19], T. Terasawa[40], S. Torii[3], Y. Tsunesada[41], Y. Uchihori[42], E. Vannuccini[2], J. P. Wefel[15], K. Yamaoka[43], S. Yanagita[44], A. Yoshida[38], K. Yoshida[22], and W. V. Zober[8]

[1]Department of Physics, University of Florence, Via Sansone, 1, 50019 Sesto, Fiorentino, Italy, [2]INFN Sezione di Florence, Via Sansone, 1, 50019 Sesto, Fiorentino, Italy, [3]Waseda Research Institute for Science and Engineering, Waseda University, 17 Kikuicho, Shinjuku, Tokyo 162-0044, Japan, [4]JEM Utilization Center, Human Spaceflight Technology Directorate, Japan Aerospace Exploration Agency, 2-1-1 Sengen, Tsukuba, Ibaraki 305-8505, Japan, [5]Institute for Cosmic Ray Research, The University of Tokyo, 5-1-5 Kashiwa-no-Ha, Kashiwa, Chiba 277-8582, Japan, [6]Department of Physical Sciences, Earth and Environment, University of Siena, via Roma 56, 53100 Siena, Italy, [7]INFN Sezione di Pisa, Polo Fibonacci, Largo B. Pontecorvo, 3, 56127 Pisa, Italy, [8]Department of Physics and McDonnell Center for the Space Sciences, Washington University, One Brookings Drive, St. Louis, Missouri 63130-4899, USA, [9]Heliospheric Physics Laboratory, NASA/GSFC, Greenbelt, Maryland 20771, USA, [10]Department of Physics, Catholic University of America, Washington, DC 20064, USA, [11]Center for Space Sciences and Technology, University of Maryland, Baltimore County, 1000 Hilltop Circle, Baltimore, Maryland 21250, USA, [12]Astroparticle Physics Laboratory, NASA/GSFC, Greenbelt, Maryland 20771, USA, [13]Center for Research and Exploration in Space Sciences and Technology, NASA/GSFC, Greenbelt, Maryland 20771, USA, [14]Institute of Applied Physics (IFAC), National Research Council (CNR), Via Madonna del Piano, 10, 50019 Sesto, Fiorentino, Italy, [15]Department of Physics and Astronomy, Louisiana State University, 202 Nicholson Hall, Baton Rouge, Louisiana 70803, USA, [16]Department of Physics and Astronomy, University of Padova, Via Marzolo, 8, 35131 Padova, Italy, [17]INFN Sezione di Padova, Via Marzolo, 8, 35131 Padova, Italy, [18]Institute of Space and Astronautical Science, Japan Aerospace Exploration Agency, 3-1-1 Yoshinodai, Chuo, Sagamihara, Kanagawa 252-5210, Japan, [19]Kanagawa University, 3-27-1 Rokkakubashi, Kanagawa, Yokohama, Kanagawa 221-8686, Japan, [20]Faculty of Science and Technology, Graduate School of Science and Technology,, Hirosaki University, 3, Bunkyo, Hirosaki, Aomori 036-8561, Japan, [21]Yukawa Institute for Theoretical Physics, Kyoto University, Kitashirakawa Oiwakecho, Sakyo, Kyoto 606-8502, Japan, [22]Department of Electronic Information Systems, Shibaura Institute of Technology, 307 Fukasaku, Minuma, Saitama 337-8570, Japan, [23]School of Advanced Science and Engineering, Waseda University, 3-4-1 Okubo, Shinjuku, Tokyo 169-8555, Japan, [24]National Institute of Polar Research, 10-3, Midori-cho, Tachikawa, Tokyo 190-8518, Japan, [25]Faculty of Engineering, Division of Intelligent Systems Engineering, Yokohama National University, 79-5 Tokiwadai, Hodogaya, Yokohama 240-8501, Japan, [26]Faculty of Science, Shinshu University, 3-1-1 Asahi, Matsumoto, Nagano 390-8621, Japan, [27]Hakubi Center, Kyoto University, Yoshida Honmachi, Sakyo-ku, Kyoto 606-8501, Japan, [28]Department of Astronomy, Graduate School of Science, Kyoto University, Kitashirakawa Oiwake-cho, Sakyo-ku, Kyoto 606-8502, Japan, [29]Institute of Particle and Nuclear Studies, High Energy Accelerator Research Organization, 1-1 Oho, Tsukuba, Ibaraki 305-0801, Japan, [30]University of Pisa, Polo Fibonacci, Largo B. Pontecorvo, 3, 56127 Pisa, Italy, [31]Astroparticle Physics Laboratory, NASA/GSFC, Greenbelt, Maryland 20771, USA, [32]Department of Electrical and Electronic Systems Engineering, National Institute of Technology, Ibaraki College, 866 Nakane, Hitachinaka, Ibaraki 312-8508, Japan [33]Department of Astronomy, University of Maryland, College Park, Maryland 20742, USA, [34]Department of Physical Sciences, College of Science and Engineering, Ritsumeikan University, Shiga 525-8577, Japan, [35]Faculty of Science and Engineering, Global Center for Science and Engineering, Waseda University, 3-4-1 Okubo, Shinjuku, Tokyo 169-8555, Japan, [36]Department of Physics and Astronomy, University of Denver, Physics Building, Room 211, 2112 East Wesley Avenue, Denver, Colorado 80208-6900, USA, [37]Quantum ICT Advanced Development Center, National Institute of Information and Communications Technology, 4-2-1 Nukui-Kitamachi, Koganei, Tokyo 184-8795, Japan, [38]College of Science and Engineering, Department of Physics and Mathematics, Aoyama Gakuin University, 5-10-1 Fuchinobe, Chuo, Sagamihara, Kanagawa 252-5258, Japan, [39]College of Industrial Technology, Nihon University, 1-2-1 Izumi, Narashino, Chiba 275-8575, Japan [40]RIKEN, 2-1 Hirosawa, Wako, Saitama 351-0198, Japan, [41]Division of Mathematics and Physics, Graduate School of Science, Osaka City University, 3-3-138 Sugimoto, Sumiyoshi, Osaka 558-8585, Japan, [42]National Institutes for Quantum and Radiation Science and Technology, 4-9-1 Anagawa, Inage, Chiba 263-8555, Japan, [43]Nagoya University, Furo, Chikusa, Nagoya 464-8601, Japan, [44]College of Science, Ibaraki University, 2-1-1 Bunkyo, Mito, Ibaraki 310-8512, Japan